Surface erosion of soil: Testing methods and applications

Yunjie Lin & Cheng Lin
Department of Civil Engineering – University of Victoria, Victoria, British Columbia, Canada

GeoCalgary 2022 October 2-5
Reflection on Resources

ABSTRACT
Surface erosion refers to scouring the exterior surface of soil. Soil grains are removed by flowing fluid during the erosion process. Surface erosion has now been recognized as one of the major concerns of infrastructures which interact with water, such as bridges, dams, quays, and levees. Thus, there is a growing need for a better understanding of soil erosion and testing methods. In the past half-century, various apparatuses have been developed to investigate the surface erosion behavior of different soils. This paper reviews the existing apparatuses to create a compressive picture of available testing methods for soil surface erosion. By comparing the principles, features, and limitations, we discuss the feasibility of each methodology. We also discussed the effect of soil/fluid properties on the erodibility of soil and addressed the research gap of coupled physiochemical effects of eroding fluids on soil erosion. Furthermore, we present the developed Countertop Surface Erosion Apparatus to fulfill the research need.

RÉSUMÉ
L'érosion de surface fait référence à l'affouillement de la surface extérieure du sol. Les grains de sol sont enlevés par l'écoulement des fluides pendant le processus d'érosion. L'érosion de surface est maintenant reconnue comme l'une des préoccupations majeures des infrastructures liées à l'eau, telles que les ponts, les barrages, les quais et les digues. Ainsi, il est de plus en plus nécessaire de mieux comprendre l'érosion des sols et les méthodes d'essai. Au cours du dernier demi-siècle, divers appareils ont été développés pour étudier le comportement d'érosion de surface de différents sols. Cet article passe en revue les appareils existants pour créer une image compressive des méthodes d'essai disponibles pour l'érosion de la surface du sol. En comparant les principes, les fonctionnalités et les limites, nous discutons de la faisabilité de chaque méthodologie. Nous avons également discuté de l'effet des propriétés sol/fluide sur l'érodabilité du sol et abordé le manque de recherche des effets physicochimiques couplés des fluides érosifs sur l'érosion du sol. De plus, nous présentons l'appareil d'érosion de surface de comptoir développé pour répondre au besoin de recherche.

1 INTRODUCTION

Surface erosion of soil is a process of transporting soil grains by flowing fluid. It has now been recognized as one of the major concerns of water-related infrastructures, such as bridges, quays, and levees. According to a survey of more than 1000 bridge failures in the United States, failures caused by erosion occupied 60%, which is 30 times those caused by earthquakes (Shirole and Holt 1991). Removal of soil around bridge foundations leads to a reduction of soil support to structure, and thus diminishes the capacity of the foundation (Lin and Lin 2019; 2020). Overtopping due to the water spilling and surface erosion leads to more than 30% of dam failures (Costa et al. 1985). Breaching of the embankment occurs in short and can cause severe flood events downstream.

Currently, the excess shear stress equation, shown in Eq. 1, is widely accepted for erosion analyses, which recognizes the hydraulic shear stress (τ) at the soil-water interface as the erosive force (Williamson and Ockenden 1996; Reddi et al. 2000; Briaud et al. 2001; 2017; Wan and Fell 2004).

$$\dot{\varepsilon} = K_d(\tau - \tau_c)^n \quad [1]$$

where $\dot{\varepsilon}$ is the erosion rate; K_d is the erodibility index, and τ_c is the critical shear stress.

Erosion occurs once the hydraulic erosive force (τ) exceeds the threshold (τ_c). Resistive force against erosion varies between cohesionless soil and cohesive soil. Briaud et al. (2001) revealed that the erodibility of sands and gravels is governed by gravitational force and frictions between adjacent particles. Based on experimental investigation using slow-motion videotapes, it was concluded that sliding and rolling are two main mechanisms of erosion of cohesionless soils. Erosion of cohesive soils is more complex as electromagnetic and electrostatic forces play an important role in resisting erosion. Electrical interactions between clay particles involve attractive force and repulsive force. The former mainly refers to the Van der Waal force which varies inversely with the third or fourth order of the distance between particles. The repulsive force is dominated by the properties of the double layer water according to the Guoy-Chapman theory. Repulsive forces are affected by many factors, such as cation concentration, ionic valence, and temperature.

In the past half-century, many apparatuses have been developed for surface erosion testing. This paper summarized four laboratory erosion testing methods. Principles, features, limitations, and applications of each

category are discussed to provide recommendations for selecting the erosion testing method. We also discussed the effect of soil/fluid properties on the erodibility of soil and addressed the research gap of coupled physiochemical effects of eroding fluids on soil erosion. Furthermore, the development of Countertop Surface Erosion Apparatus (CSEA) is presented.

2 EXISTING SURFACE EROSION TESTING METHODS

Based on the excess shear stress analyzing method, as shown in Eq. 1, numerous apparatuses were developed for laboratory erosion testing. The hydraulic shear stress on the soil-water boundary is estimated or directly measured, while eroded soil particles are collected within a certain period for erosion analysis. The key testing sections of existing apparatuses mainly include four types: flume, closed conduit, submerged jetting, and rotating cylinder. Principles, features, and drawbacks of each category of erosion testing apparatus are discussed in the following subsections. The feasibility of each testing method is also discussed.

2.1 Flume

Flumes of different sizes and shapes have been constructed to investigate soil erosion caused by the open channel flow. Erosion flumes usually need to be sufficiently long to fully develop the flow before the testing section, as shown in Figure 1. Kandiah and Arulanladan (1974) developed a straight flume for erosion testing: length of the flume, L_F = 2.5m; width of the flume, W_F = 0.15m and height of the flume, H_F = 0.3m. The flume was connected to a pump and reservoirs to generate water flow. The height of the flow was adjusted by a head gate and a tail gate at ends of the flume and flow velocity was controlled and measured through a valve and flow meter. Remolded samples were placed at the bottom and inserted into the flume through the opening for erosion as shown in Figure 1a. The flowing water can thus generate shear stress up to 8.5 Pa in their research.

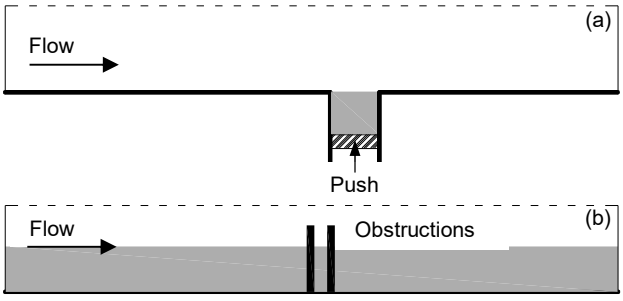

Figure 1. Straight flumes for erosion testing

The induced hydraulic shear stress on the soil-water boundary, however, is difficult to measure. Kandiah and Arulanladan (1974) used a Preston tube for the measurement, which is essentially a Pitot tube that consists of a circular pipe (d_p). The Preston tube was inserted beneath the water surface and was put close to the sample surface, with the opening facing upstream. By comparing the reading of total pressure (p_t) and statistic pressure (p_s), the shear stress can be calculated using Eq. 2 (Preston 1954):

$$\log\frac{\tau {d_p}^2}{4\rho\nu^2} = -2.604 + \frac{7}{8}\log\frac{(p_t - p_s)}{4\rho\nu^2}{d_p}^2 \quad [2]$$

where d_p is the diameter of the Pitot tube, ρ is the density of eroding fluid and ν is the kinematic viscosity.

However, this method became unreliable if the left part in Eq. 2 falls out of the region 4.5-6.5. The Pitot tube also rested within the laminar sublayer, which to some extent, caused disturbance to the flow nearby the boundary. Instead of measuring shear stress at the top surface of the sample, Shan et al. (2005) designed a direct force gauge for their ex-situ scouring testing device (ESTD) which sat beneath the sample. A testing sample with a diameter of 63.5 mm and a maximum height of 15 mm was fixed to a sensor disk. During the test, as flow applied shear force to the sample surface, horizontal deflection of the sample was captured by the sensor disk. The signal was transferred, amplified, and translated into the corresponding force within the electromagnetic field inside the force gauge.

The open channel flume is also featured to investigate erosion around obstructions, as presented in Figure 1b. Tao et al. (2018) developed a flume of similar length and height, but with a doubled width (W_F = 0.3m) to study the scour around bridge piers, which is now recognized as the major reason of bridge failures. A uniform sand layer was placed across the flume bed and different shaped pier models were embedded in soil for testing. It needs to be noted that the boundary effect is critical to be considered especially for narrow flumes. For example, a wider flume is needed to avoid the wall effect due to the block of the pier to the flow. According to Amini et al. (2012), the block ratio (blocked width/flume width) should be smaller than 12%, while Raudkivi and Ettema (1983) suggested a value of 16%. Other recommendations for flume dimensions are also summarized in Table 1 (Amini et al. 2012; Raudkivi and Ettema 1983; Cardoso et al. 1989; Raju et al. 2000; Melville and Coleman, 2000).

Table 1. Dimension requirements for straight flume design

Index	Recommendation
Block ratio	$\frac{W_p}{W_F} < 12\%\ or\ 16\%$
Flow length and flow depth	$50 < \frac{L_F}{h_{flow}} < 150$ $\frac{h_{flow}}{W_p} \geq 3.5$
Sediment size	$\frac{W_p}{D_{50}} < 50$

where W_F and L_F are the width and length of the flume, respectively, W_p is the pier width, h_{flow} is the flow depth, and D_{50} is the median particle size of soil

2.2 Closed conduit

Different from flumes, erosion apparatus with closed conduit adopts a narrow and enclosed testing section, as shown in Figure 2. The cross-section of the conduit is usually rectangular with an opening for inserting testing soil samples. Eroding fluid is circulated by a water pump within the system, and the velocity of flow is controlled for erosion tests. McNeil et al. (1996) designed the SEDFlume (sediment erosion at depth flume) at the University of Santa Barbara for erosion testing with applied shear stress up to 10 Pa. It was assumed that particulate erosion (i.e., individual grains are resuspended and scoured) mainly occurs in this range of shear stress. The conduit has a cross-section of 10×2 cm and the end of the channel has a 15 cm long opening which is connected to a soil sampler. In the inlet section of the conduit, before the opening where the soil surface is exposed to fluid, there exists a 120 cm long straight section which is sufficient to straighten the flow and assure the turbulent flow is fully developed. Briaud et al. (2001) selected a larger size of conduit to develop the EFA (Erosion Function Apparatus) with the cross-section dimensions of 101.6×50.8 mm. The conduit was connected to a Shelby tube with a diameter of 76.2 mm that contained either remolded soil or in-situ soil collected from the field. Soil sample was manually pushed into the chamber, and exposed to eroding fluid with velocity up to 6 m/s.

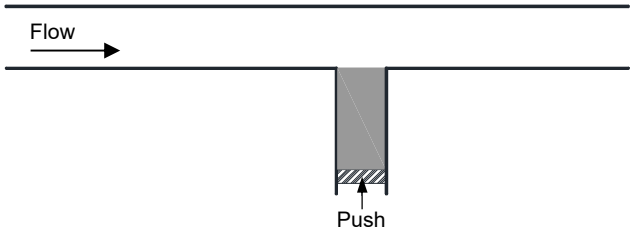

Figure 2. Closed conduit for erosion testing

During the test, the flow velocity was measured using a flow meter and the length of the eroded soil sample was recorded for a certain period at each stage of flow velocities, which indicates the erosion rate. The shear stress applied to the soil surface is calculated using the Darcy-Weisbach equation, Eq. 3-5:

$$\tau = \frac{1}{8} f \rho \bar{U}^2 \quad [3]$$

$$f = \frac{64}{R_e} \text{ for laminar flow} \quad [4]$$

$$\frac{1}{\sqrt{f}} = -2 \log\left(\frac{\epsilon/D}{3.7} + \frac{2.51}{R_e\sqrt{f}}\right) \text{ for turbulent flow} \quad [5]$$

where $\bar{U}$ is the mean flow velocity, R_e is Reynold's number which equals $\bar{U}D/\upsilon$, ϵ is the roughness of the internal pipe surface, D is the internal diameter of the pipe and f is the friction factor that can either be calculated using Eq. 4-5 or estimated using Moody chart (Moody 1944).

Compared with flume, closed conduit generates higher shear stress on the sample surface (up to 300 Pa). Thus, it can also be utilized to test a broad range of earth materials including cohesive soil, non-cohesive soil, and even soft rocks (Briaud et al. 2019). The testing soil can also represent its in-situ state as it is directly collected from the field and inserted into the conduit for testing, which minimizes the disturbance effect. Moreover, as the collected soil sample is continuously pushed into the chamber for testing, the erosion behavior of soil at different depths can be evaluated provided that a sample can be recovered.

However, estimating the roughness (ϵ) of the soil surface for calculating the friction factor (f) is challenging. Briaud et al. (2001) assumed half the particle extruded into the fluid while the other half was still embedded in the sample. Half of the median grain size was then used as the surface roughness ($\epsilon = D_{50}/2$). However, during the erosion test, the sample surface may not be eroded simultaneously which causes higher surface roughness, leading to an inaccurate estimation of shear stress. Moreover, due to the limited size of the conduit and sampler, soil with large particles cannot be tested using closed conduit apparatus. Specifically, for EFA, soil with particles greater than 40 mm cannot be tested with confidence (Briaud et al. 2019).

2.3 Submerged jetting

Instead of generating flow parallel to the sample surface, the submerged jetting erosion testing apparatus generates impingement perpendicular to the soil surface for erosion testing, as shown in Figure 3. The JET developed by Moore and Masch (1962) includes a jet tube (25.4 mm in diameter) and a submergence tank (0.915×0.915×0.458 m), which contains a soil sample. The jet tube was connected to an adjustable head tank which provided a head difference between water levels of the jet tube and the submergence tank. The lower end of the jet tube was fitted with nozzles with different openings (d_0 =4.76, 9.53, 15.88 mm) which was mounted over the sample. Hanson and Hunt (2007) developed a similar sized impinging jet for erosion testing which included a jet tube with the internal diameter of 50 mm, a nozzle with a 6.4 mm opening and a submergence tank (305 mm in diameter and 305 mm in height). Additionally, a deflection plate was also attached to the jet tube for deflecting the jet and protecting the sample surface during the initial water filling in the tank.

During the erosion testing using impinging jet, the nozzle is open, and a vertical impingement is generated which travels downward and flushes the surface of the soil sample below. Scour depth is then measured to calculate the erosion rate. The travel of the impingement can be divided into four regions (i.e., potential cone; free jet zone; impingement zone and wall jet zone), as shown in Figure 4 (Hanson and Cook, 2004; Rajaratnam and Mazurek, 2005). The flow velocity is considered as a constant (U_0) at

the nozzle, which equals $\sqrt{2gh}$, where h is the head difference between the jet tube and the submergence tank. At the perimeter of the nozzle, a turbulent shear layer develops as the jet interacts with the surrounding water within the submergence tank. The shear layer grows transversely as the impinging jet travels downward, as shown in Figure 4. Below the nozzle, there exists a natural cone which extends to a depth of $C_d d_0$, where C_d is the diffusion coefficient and d_0 is the opening diameter of the nozzle. Within the potential cone, the flow remains at a constant velocity (i.e., U_0). According to Beltaos and Rajaratnam (1974), C_d varies from 5.8-7.3 and the average value of 6.3 is commonly used in practice. As the jet travels downward, the velocity decreases as the jet continuously spreads in the transverse direction. The centerline velocity of the jet in the free jet zone can be calculated using Eq. 6 (Beltaos and Rajaratnam,1974).

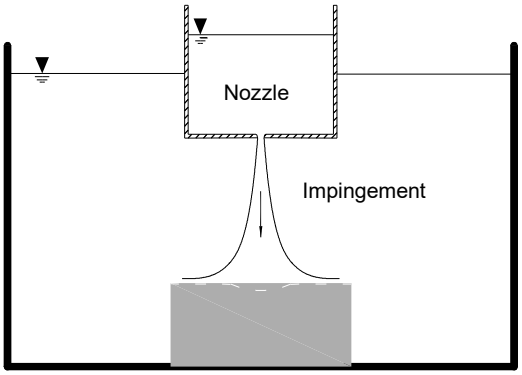

Figure 3. Submerged jetting for erosion testing

As the jet approaches the surface of the sample, the surface begins to affect the jet in the impingement zone, which is approximately located $0.86J_i$ below the nozzle (Cossette 2016). Due to the existence of the boundary surface, the centerline velocity of the jet gradually decays to zero on the top of the sample surface and in return, results in a wall pressure. During the impinging process, the vertical stream gradually turns to a direction that is parallel to the surface of the soil sample, which is known as the wall jet zone in Figure 4. The boundary of the impingement zone and the wall jet zone is located at $0.22J_i$ away from the centerline (Cossette 2016). The wall shear stress distribution is also presented in Figure 4 and the maximum shear stress can be calculated using Eq. 7, which occurs at $0.14J_i$ away from the centerline.

Hanson and Cook (2004) made the following two assumptions for jet erosion analyses: (1) In the impingement zone, the velocity still decays like a free jet. In other words, by neglecting the effect of the boundary surface, the velocity relationship given by Beltaos and Rajaratnam (Eq. 6) still applies in the impingement zone. (2) The maximum scour depth developed in the soil sample is due to the maximum shear stress.

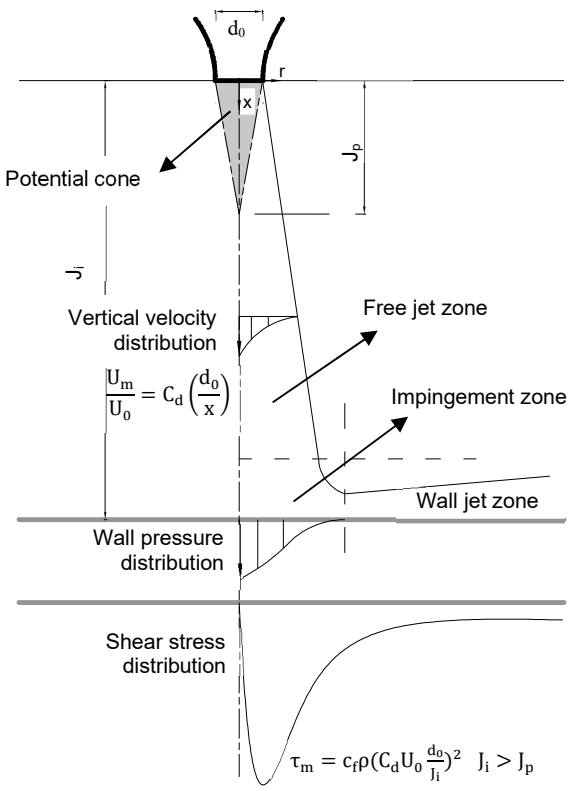

Figure 4. Schematic of the vertical impinging jet (Modified from Rajaratnam and Mazurek 2005 & Hanson and Cook 2004)

$$\frac{U_m}{U_0} = C_d \frac{d_0}{x} \quad [6]$$

$$\tau_m = C_f \rho {U_m}^2 \quad [7]$$

$$\tau_m = C_f\rho(C_d U_0 \frac{d_0}{J_i})^2 \qquad x > J_p \quad [8]$$

Where x is the distance away from the nozzle and U_m is the maximum velocity at the distance of x. τ_m and U_m are the maximum shear stress and maximum velocity at a distance x, respectively.

Combining Eq. 6 and 7, the maximum boundary shear stress below the potential cone can be calculated based on the first assumption. With Eq. 8, operators can estimate the shear stress in need for a specific soil sample and determine the device setup such as the nozzle size (d_0), head difference (h) and the distance between nozzle and sample surface (J_i).

As the jet erosion processes with time, the erosion rate (dx/dt) is assumed as a function of maximum shear stress at the boundary based on the second assumption. The erosion process eventually ends up once the equilibrium scour depth (J_e) has been reached, which corresponds to

the critical state of soil (i.e., critical shear stress τ_c). The critical shear stress (τ_c) can be calculated by substituting the equilibrium scour depth J_e to J_i in Eq. 8. However, during the erosion test, it is very difficult to achieve the equilibrium state, especially for cohesive soil. Consequently, the maximum scour depth at equilibrium is usually estimated (Hanson and Cook 2004).

Compared with flume and closed conduit, submerged jetting is relatively inexpensive. However, the analyses of impinging jet erosion testing are based on the assumptions as discussed previously and thus, lead to uncertainties. The shear stress is non-uniformly distributed as shown in Figure 4, but the analysis is only based on the peak shear stress. Moreover, there exists different methods for estimating critical shear stress (τ_c), that produce significantly different results which may lead to confusion in practice (Cossette 2016). The submerged jetting method is also limited to soils without large particles due to the limited sample size. Coarse-grained materials with particles larger than 30 mm cannot be tested, as it tends to fall back into the scour hole due to gravity (Briaud et al. 2019).

2.4 Rotating cylinders

Inspired by viscometers, Moore and Masch (1962) developed a rotating cylinder apparatus for erosion testing at the University of Texas, which enabled accurate direct measurement of hydraulic shear stress applied on the sample surface. A cylindrical sample (D_s = 76.2mm, H_s =66.2 mm), secured with plates and a cross-sample pivot, is coaxially mounted into a slightly larger transparent cylinder, as shown in Figure 5. The annular space between the sample and the outer cylinder is filled with eroding fluid and a motor is mounted at the bottom of the transparent cylinder which can drive the cylinder to speed up to 2500 RPM. Fluid in the annulus is driven by the chamber as it rotates during the test, which induces hydraulic shear stress on the sample surface.

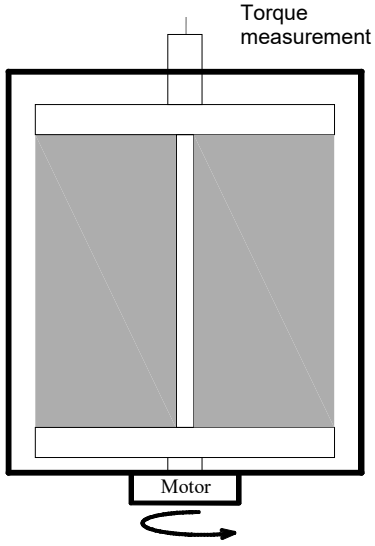

Figure 5. Rotating cylinders for erosion testing

The principle of the device is to measure the torque that holds the soil sample stationary when exposed to the rotational flow during erosion testing. The protrusion of the center pivot is connected to a torque indicator in the erosion device. During the test, the sample remains still, and the hydraulic shear stress applied on the sample surface is represented and calculated by the torque reading using Eq. 9. The erosion rate can be obtained by collecting and weighing eroded soils at each testing stage.

$$\tau = \frac{T}{2\pi {R_s}^2 H_s} \quad [9]$$

where T is the torque measured during the test, R_s and H_s are the radius and height of the sample, respectively.

Recently, the design of rotating cylinders has been adopted and improved by many researchers for erosion testing. Chapuis and Gatien (1985) removed the middle pivot. Instead, sample plates were guided in rotation by ball bearings and rotated freely relative to the transparent cylinder. It was found that for the same rotating speed, the torque captured by the sensor was not consistent. It could be attributed to the surface roughness change during the erosion test. To accurately manipulate the shear stress that is applied to the sample surface, Bloomquist et al. (2012) introduced a control /monitoring system. The rotational speed was continuously adjusted to maintain a constant torque reading.

Different from pump driven device in which the water flow is interrupted by a water pump, rotating cylinders generate infinite flow length which eases the development of flow. Rotational annulus flow also generates more uniform shear stress on the sample surface for erosion testing, as compared with other devices as presented foregoing. However, the testing sample needs to be self-stable when submerged in water.

3 APPLICATIONS OF EXISTING METHODS

The existing four types of laboratory erosion testing methods are developed based on different principles and measuring methods. These methods have different features and limitations and thus have different applications. In this section, selection of erosion testing methods for different soils is discussed. Experimental outcomes and the current research gap are also discussed.

Different testing methods achieve a different range of flow conditions for erosion testing. The open flume (Figure 1a) achieves the lowest hydraulic shear stress (up to 15Pa) on the soil/water interface. The reason is that: the flume usually has a large setup to avoid the scale effect. As such, a large amount of fluid is needed for erosion testing, which is harder to be driven to a high flow rate. Closed conduit, on the contrary, achieves the highest level of shear stress (up to 351.25 Pa). The cross-section area is small, so the flow inside can achieve a very high speed (up to 6 m/s), compared with a large open flume. Rotating cylinders and impinging jet generate relatively low shear stress, which is still sufficient for erosion testing for most geo-materials.

Briaud et al. (2017) proposed an erosion chart based on testing results using Erosion Function Apparatus (Closed conduit). Geomaterials are classified into six scenarios based on erodibility. Combining the achievable shear stress of each testing method, Table 2 summarized the feasibility of each testing method for different types of soil. The closed conduit is compatible with most of the geo-materials, even suitable for soft rocks. Rotating cylinder, however, is limited to III and IV class cohesive soils, as it requires the testing sample to be self-stable when submerged in water.

Table 2. Feasibility chart of existing erosion testing methods

Erosion testing method	Soil type					
	SM SP	ML	MH CL	CH	Rock	
Flume						
Closed conduit						
Submerged jetting						
Rotating cylinder						
	I	II	III	IV	V	VI
	Erodibility class					

Unique features of the apparatuses also need to be considered when selecting the erosion testing method, as shown in Table 3. Flume simulates the open channel flow and thus can be applied for testing erosion caused by river flow. To simulates the log-law velocity profile of natural open channel flow, Shan et al. (2015) mounted a moving belt with peddles to the top of the flume to manipulate the velocity profile for erosion experiments. Moreover, flume is also featured of erosion tests considering water-structure interaction, as shown in Figure 1b. Sumer et al. (2005) investigated used a flume to investigate local and global scour developed around pile groups. Scaled pile groups were embedded in a layer of sand for testing. Downflow, horseshoe vortex and wake vortices are generated when the water flow interacted with the structure and generated scour holes around pile groups. Closed conduit such as the Erosion Function Apparatus (EFA) proposed by Briaud et al. (2001) is compatible with Shelby tube. Thus, this type of apparatus is featured of testing in-situ status soil samples at different depths. The submerged jetting method can be used for in-situ testing directly, due to the easy device setup. Hanson and Cook (2004) presented an in-situ impinging jet apparatus. The submergence tank for in-situ testing has openings on both ends, which is driven into the soil bed before the test. Eroding fluid was obtained nearby the testing site and was pumped into the head tank. Vertical jet was created through the nozzle, impinging towards the soil. The excess water during the test came out from the submergence tank through the opening at the top. The in-situ impinging jet erosion can be performed on a slope as well, which has an angle smaller than 26° (Briaud et al. 2019). The design of Rotating cylinders is known for the capability of direct and accurate measurement, as mentioned before. Shear stress is indicated by the torque, which can be measured by a thin brass torsional rod, pulley-weight system, torsion spring and strain gauge or torque cell (Shen and Akky 1974; Chapuis and Gatien 1986; Lim and Khalili 2009; Bloomquist et al. 2012).

Table 3. Unique features of existing surface erosion testing methods

Erosion testing method	Unique features
Flume	Simulates river flow Considers water-structure interaction
Closed conduit	Compatible with most geomaterials Compatible with in-situ status sample
Submerged jetting	Capable of in-situ erosion testing
Rotating cylinder	Directly measures shear stress

With the erosion testing methods, many laboratory tests have been conducted to investigate the erodibility of soil with different properties. It was found that the critical shear stress of sands and gravels is proportional to the average diameter of particles (Briaud et al. 2001). An increase in the fine content increases the erosion resistance (Scholtès 2010; Tian et al. 2020). Furthermore, the erodibility is also related to the geo-properties of soil. Soil compacted to higher dry density and to the wet side of optimum moisture content has higher erosion resistance (Wan and Fell 2004). An increase in plasticity index (PI) and undrained shear stress S_u leads to higher erosion resistance (Briaud et al. 2019). Recently, there is a growing recognition of the effects of physicochemical properties of eroding fluid. Based on flume tests, Wynn and Mostaghimi (2006) revealed that a 2 ℃ increase in water temperature increased the erosion rate by 30%. The critical shear stress for erosion increased with the salinity of eroding fluid (Kelly and Gularte 1981). Moreover, it was also found that an increasing salt concentration reduced the erosion rate (Kandiah and Arulanandan 1974; Reddi et al. 2000). Other chemical properties such as pH value which changes the clay particle charge and dispersion behavior, are, however, rarely considered in erosion studies. Moreover, the coupled physicochemical effects of fluids on soil erosion have rarely been investigated in previous research. Thus, there is a need for research efforts to improve the understanding of soil erosion under different hydraulic conditions.

However, most of the existing surface erosion devices cannot fulfill the research need. Water flow inside the flumes and closed conduit is usually circulated by a water pump, which involves thermal conduction during the test, leading to difficulties in temperature control. For example, for a typical erosion test using EFA, the water temperature increased from 16℃ to 34℃ (Al-Ali 2016). Furthermore, chemical solutions may also degrade the water systems of existing erosion apparatus.

4 DEVELOPMENT OF CSEA

To fulfill the research gap in investigating coupled physiochemical effects of eroding fluids on soil erosion, the

Countertop Surface Erosion Apparatus (CSEA) is developed at the University of Victoria. The apparatus adopts the design of rotating cylinders as it enables direct measurement of shear stress and eases the control of fluid properties due to the small-scale setup.

Figure 6 shows the assembly of CSEA, which mainly consists of a motor and a cylindrical testing chamber, supported by shafts and posts. The rotating chamber includes a transparent Lexan tube, containment top and base. Chamber dimensions were determined based on Computational Fluid Dynamics (CFD) analyses to minimize the effect of secondary flow such as Taylor vortexes. The testing soil sample can be either compacted or recovered with a Shelby tube. Instead of using a cross-sample pivot, shown in Figure 5, the sample is secured by sample plates and a compression spring. Motions of the sample set, and the chamber are disassociated by sealed ball bearings.

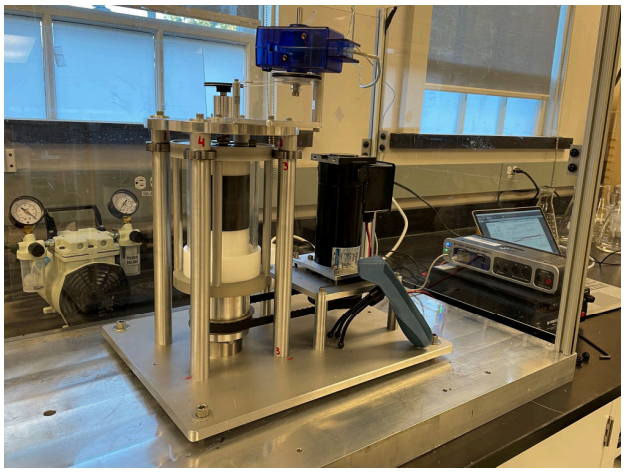

Figure 6. Countertop Surface Erosion Apparatus (CSEA)

The outer Lexan tube, as well as containment plates, are spined by a 1/3 hp DC motor, through a belt-driven transmission system. The motor rotates up to 3900 RPM and is controlled by changing voltage output in the DC power supply (BK Precision 1901B). The rotational speed of the chamber is measured using a non-contact tachometer, as shown in Figure 6. As the chamber rotates, rotational annulus flow induces hydraulic shear stress on the sample surface. The torque caused by the shear stress is captured by the torque measurement assembly mounted on the top of the device, which includes pulley wheels, string, tension spring and a rotary motion sensor (PASPORT PS-2120A). After erosion tests, the eroded soil particles are collected and weighed to calculate the erosion rate for analysis.

To be compatible with erosive chemical solutions for studying physiochemical effects of eroding fluids, corrosion-resistant materials, such as acrylic plastic and Delrin plastic, were selected to manufacture the chamber and sample plates of CSEA. Figure 7 shows the temperature change of fluid for erosion testing using CSEA at 500, 1000 and 1500 RPMs. It can be concluded that for a typical 2-min erosion testing using CSEA, the fluid temperature change is less than 1℃. As compared with pump driven devices which experience up to 17℃ fluid temperature rise during the test, the developed CSEA minimizes the temperature change of eroding fluid.

The ongoing research evaluates the fluid properties effect on soil erosion. The temperature of prepared solutions is controlled using an external water bath before erosion tests. Furthermore, a working environment is also in development to reduce the thermal conduction between the eroding fluid and ambience.

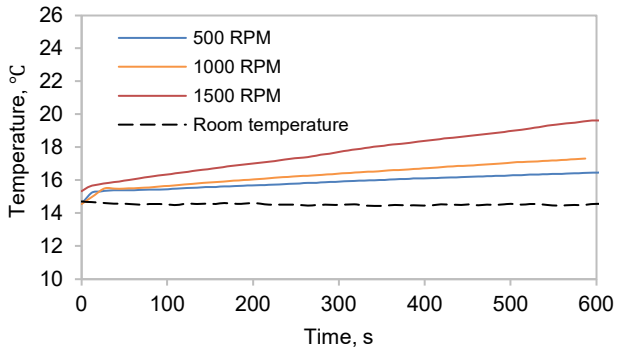

Figure 7. The temperature change of fluid during tests

5 CONCLUSIONS

In this paper, the existing laboratory surface erosion testing methods were summarized into four categories. The device setup, testing principle, measuring methods and limitations are presented to give an overview of the available methodology for surface erosion testing. By comparing the simulated hydraulic conditions, a feasibility chart is presented to provide guidelines for selecting an appropriate testing method for different types of soil. Unique features of each method are also highlighted to address specific testing requirements. Furthermore, a new testing apparatus, Countertop Surface Erosion Apparatus (CSEA), developed at the University of Victoria is presented. The developed CSEA is compatible with intact soil samples and corrosive eroding fluid for erosion testing. The narrow chamber design based on CFD analyses reduces the effect of Taylor vortexes and achieves more uniform hydraulic shear stress on the sample surface, which can be directly measured during tests. The ongoing research at the University of Victoria using the developed CSEA focuses on the coupled effects of fluid properties, which will contribute to the understanding of soil erosion under various hydraulic conditions.

REFERENCES

Al-Ali, A.M.A., 2016. Temperature effects on fine-grained soil erodibility, MSc thesis, Kansas State University.

Amini, A., Melville, B.W., Ali, T.M. and Ghazali, A.H. 2012. Clear-water local scour around pile groups in shallow-water flow, *Journal of Hydraulic Engineering*, 138(2): 177-185.

Beltaos, S. and Rajaratnam, N. 1974. Impinging circular turbulent jets, *Journal of the hydraulics division*, 100(10): 1313-1328.

Bloomquist, D., Sheppard, D.M., Schofield, S. and Crowley, R.W. 2012. The rotating erosion testing apparatus (RETA): A laboratory device for measuring erosion rates versus shear stresses of rock and cohesive materials, *Geotechnical Testing Journal*, 35(4): 641-648.

Briaud, J.L., Ting, F.C.K., Chen, H.C., Cao, Y., Han, S.W. and Kwak, K.W. 2001. Erosion function apparatus for scour rate predictions, *Journal of geotechnical and geoenvironmental engineering*, 127(2): 105-113.

Briaud, J.L., Govindasamy, A.V. and Shafii, I. 2017. Erosion charts for selected geomaterials, *Journal of geotechnical and geoenvironmental engineering*, 143(10): 04017072.

Briaud, J.L., Shafii, I., Chen, H.C. and Medina-Cetina, Z. 2019. *Relationship between erodibility and properties of soils*, The National Academies Press, Washington, D.C., USA.

Cardoso, A.H., Graf, W.H. and Gust, G. 1989. Uniform flow in a smooth open channel, *Journal of Hydraulic Research*, 27(5): 603-616.

Chapuis, R.P. and Gatien, T. 1986. An improved rotating cylinder technique for quantitative measurements of the scour resistance of clays, *Canadian geotechnical journal*, 23(1): 83-87.

Cossette, D. 2016. Erodibility and scour by a vertical submerged circular turbulent impinging jet in cohesive soils, PhD dissertation, University of Saskatchewan.

Costa, J.E. 1985. Floods from dam failures, *US Geological Survey*, 85(560).

Hanson, G.J. and Cook, K.R. 2004. Apparatus, test procedures, and analytical methods to measure soil erodibility in situ, *Applied engineering in agriculture*, 20(4): 455.

Hanson, G.J. and Hunt, S.L. 2007. Lessons learned using laboratory JET method to measure soil erodibility of compacted soils, *Applied engineering in agriculture*, 23(3): 305-312.

Kandiah, A. and Arulanandan, K. 1974. Hydraulic erosion of cohesive soils, *Transportation Research Record*, 497: 60-68.

Kelly, W.E. and Gularte, R.C. 1981. Erosion resistance of cohesive soils, *Journal of the Hydraulics Division*, 107(10): 1211-1224.

Lim, S. and Khalili, N. 2009. An improved rotating cylinder test design for laboratory measurement of erosion in clayey soils, *Geotechnical testing journal*, 32(3): 1-7.

Lin, Y. and Lin, C. 2019. Effects of scour-hole dimensions on lateral behavior of piles in sands, *Computers and Geotechnics*, 111: 30-41.

Lin, Y. and Lin, C. 2020. Scour effects on lateral behavior of pile groups in sands, *Ocean Engineering*, 208: 107420.

McNeil, J., Taylor, C. and Lick, W. 1996. Measurements of erosion of undisturbed bottom sediments with depth. *Journal of Hydraulic Engineering*, 122(6): 316-324.

Melville, B.W. and Coleman, S.E. 2000. *Bridge scour*, Water Resources Publication.

Moody, L.F. 1944. Friction factors for pipe flow. *Transactions of the American Society of Mechanical Engineers*, 66: 671-684.

Moore, W.L. and Masch Jr, F.D. 1962. Experiments on the scour resistance of cohesive sediments, *Journal of Geophysical Research*, 67(4):1437-1446.

Preston, J. 1954. The determination of turbulent skin friction by means of Pitot tubes. *The Aeronautical Journal*, 58(518): 109-121.

Rajaratnam, N. and Mazurek, K.A. 2005. Impingement of circular turbulent jets on rough boundaries, *Journal of Hydraulic research*, 43(6): 689-695.

Raju, K.R., Asawa, G.L. and Mishra, H.K. 2000. Flow-establishment length in rectangular channels and ducts. *Journal of Hydraulic Engineering*, 126(7): 533-539.

Raudkivi, A.J. and Ettema, R. 1983. Clear-water scour at cylindrical piers, *Journal of hydraulic engineering*, 109(3): 338-350.

Reddi, L.N., Lee, I.M. and Bonala, M.V. 2000. Comparison of internal and surface erosion using flow pump tests on a sand-kaolinite mixture, *Geotechnical testing journal*, 23(1): 116-122.

Scholtès, L., Hicher, P.Y. and Sibille, L. 2010. Multiscale approaches to describe mechanical responses induced by particle removal in granular materials, *Comptes Rendus Mécanique*, 338(10-11): 627-638.

Shan, H., Shen, J., Kilgore, R. and Kerenyi, K. 2015. Scour in cohesive soils, *FHWA-HRT-15-033*, United States. Federal Highway Administration. Office of Infrastructure Research and Development.

Shen, C.K. and Akky, M.R. 1974. Erodibility and durability of cement-stabilized loam soil, *Transportation Research Record*, 501: 54-58.

Shirole, A.M. and Holt, R.C. 1991. Planning for a comprehensive bridge safety assurance program, *Transportation Research Record*, 1290(3950): 290-005.

Sumer, B.M., Fredsøe, J. and Bundgaard, K. 2005. Global and local scour at pile groups, The Fifteenth International Offshore and Polar Engineering Conference, OnePetro.

Tao, J., Li, J., Wang, X. and Bao, R. 2018. Nature-inspired bridge scour countermeasures: Streamlining and biocementation. *Journal of Testing and Evaluation*, 46(4): 1376-1390.

Tian, D., Xie, Q., Fu, X. and Zhang, J. 2020. Experimental study on the effect of fine contents on internal erosion in natural soil deposits, *Bulletin of Engineering Geology and the Environment*, 79(8): 4135-4150.

Wan, C.F. and Fell, R. 2004. Investigation of rate of erosion of soils in embankment dams, *Journal of geotechnical and geoenvironmental engineering*, 130(4): 373-380.

Williamson, H. and Ockenden, M. 1996. ISIS: An Instrument for Measuring Erosion Shear Stress In Situ, *Estuarine, Coastal and Shelf Science*, 42(1): 1-18.

Wynn, T. and Mostaghimi, S. 2006. The effects of vegetation and soil type on streambank erosion, southwestern Virginia, USA, *JAWRA Journal of the American Water Resources Association*, 42(1): 69-82.